CO Homologation Hot Paper

How to cite: *Angew. Chem. Int. Ed.* **2022**, *61*, e202202241
International Edition: doi.org/10.1002/anie.202202241
German Edition: doi.org/10.1002/ange.202202241

# Functionalization and Hydrogenation of Carbon Chains Derived from CO**

*Maria Batuecas, Richard Y. Kong, Andrew J. P. White, and Mark R. Crimmin**

**Abstract:** Selective reactions that combine $H_2$, CO and organic electrophiles (aldehyde, ketones, isocyanide) to form hydrogenated $C_3$ and $C_4$ carbon chains are reported. These reactions proceed by CO homologation mediated by $[W(CO)_6]$ and an aluminum(I) reductant, followed by functionalization and hydrogenation of the chain ends. A combination of kinetics (rates, KIEs) and DFT calculations has been used to gain insight into a key step which involves hydrogenation of a metal-locarbene intermediate. These findings expand the extremely small scope of systems that combine $H_2$ and CO to make well-defined products with complete control over chain length and functionality.

The controlled polymerization, hydrogenation and dehydration of $CO/H_2$ mixtures to form hydrocarbons by the Fischer–Tropsch (F–T) process is an essential reaction for industry.[1,2] There has long-been interest in controlling the selectivity of this reaction.[3] Many have advocated the potential of homogeneous catalysts to lead to reaction products with defined molecular weight and oxygen content.[4,5]

Despite these ambitions, homogeneous reactions that lead to F–T products are incredibly rare.[4,6–13] Our fundamental understanding of this type of reactivity is limited; there are only a handful of well-defined systems that combine CO and $H_2$ in a single reaction sequence to form either hydrocarbon ($C_xH_y$) or oxygenate ($C_xH_yO_z$) products. In 1991, Lippard and co-workers reported the reductive coupling and hydrogenation of CO to form *cis*-disiloxyethylene compounds, mediated by vanadium complexes.[14] More recently, Peters and Suess reported a similar product from the hydrogenation of a CO derived iron dicarbyne.[15] Hou and co-workers have documented the hydrodeoxygenative cyclotetramerization of CO by a trinuclear titanium poly(hydride) complex to form a cyclobutanone product.[16] Stephan and co-workers have shown that a simple lithium amide base ($LiNCy_2$) can react with $CO/H_2$ mixtures to form small amounts (<10 % yield) of an α-hydroxy amide derived from coupling and hydrogenation of two CO units.[17]

These systems represent the limit of knowledge in this field and have clear limitations. To date only $C_2$ and $C_4$ hydrogenated chain-growth products have been isolated. There are no examples of generating more complex products by incorporating organic electrophiles (other than CO) within the carbon chain. There is also a lack of detailed mechanistic information on the hydrogenation step. A broader scope and deeper understanding of these types of transformations could be an important factor in ultimately achieving selective F–T catalysis.

Herein, we describe the direct hydrogenation of a series of CO homologation products, including for the first time, well-defined reactivity of $C_3$ carbon chains. We show that F–T products can be obtained by reaction with CO, organic electrophiles, a main group reductant and $H_2$. We provide a mechanistic description of the key hydrogenation step, shedding light on a key C–H bond formation pathway of relevance to F–T catalysis. We have previously reported carbon-chain growth reactions from **1**, $[W(CO)_6]$ and

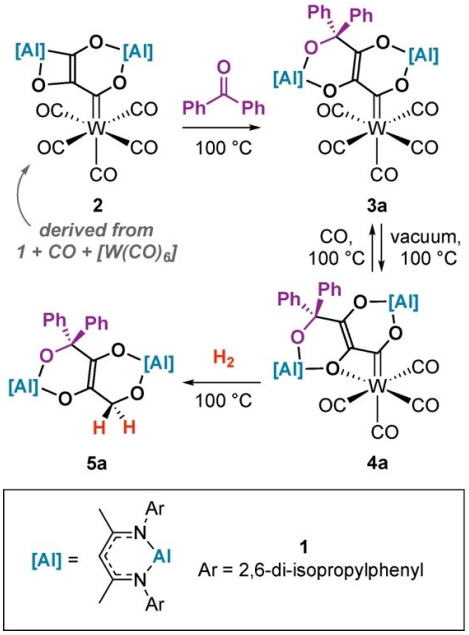


***Scheme 1.*** Reactions of **2** with benzophenone and $H_2$.

[*] Dr. M. Batuecas, Dr. R. Y. Kong, Dr. A. J. P. White, Prof. Dr. M. R. Crimmin
Department of Chemistry, MSRH, Imperial College London
82 Wood Lane, Shepherds Bush, London, W12 0BZ (UK)
E-mail: m.crimmin@imperial.ac.uk

[**] A previous version of this manuscript has been deposited on a preprint server (https://doi.org/10.26434/chemrxiv-2021-ndmfl).

CO.[18,19] Reaction of **2** with benzophenone at 100 °C in $C_6D_6$ led to the formation of **3a** and **4a** in 81 % yield, in a 4:1 ratio based on $^1$H NMR spectroscopy (Scheme 1).

The conversion of **3a** to **4a** is reversible. Heating mixtures of **3a**+**4a** under 1 atm. of CO for 12 h at 100 °C led to complete conversion to **3a**. Upon heating under vacuum, **3a** partially converts back to **4a**. DFT calculations are consistent with the reversible reaction. Formation of **4a** from **3a** was calculated to be endergonic ($\Delta G°_{298K} = +6.2$ kcal mol$^{-1}$) and occur via an interchange mechanism ($\Delta G^{+}_{298K} = +25.4$ kcal mol$^{-1}$) (Figure 1a).

Compounds **3a** and **4a** have been characterized by multinuclear NMR and IR spectroscopy. In $C_6D_6$ solution, **3a** and **4a** display $^{13}$C NMR resonances for the metallocarbene ligand at $\delta = 315.6$ and 310.9 ppm respectively. The equatorial and axial carbonyl ligands of **3a** are magnetically inequivalent and appear at $\delta = 203.3$ and 205.1 ppm. For comparison, **4a** shows three resonances for the CO ligands in the $^{13}$C NMR spectrum at $\delta = 215.5$, 218.8 and 221.4 ppm due to the reduction in symmetry. IR spectroscopy is consistent with a change in geometry around the metal center from **3a** (ν (CO) = 2050, 1897 and 1871 cm$^{-1}$) to **4a** (ν (CO) = 1988, 1874, 1862 and 1825 cm$^{-1}$) due to CO dissociation.

In the solid-state, the W–C bond length of **3a** of 2.269(4) Å is longer than that of 2.195(3) Å found in **2**. Formation of the κ$^2$-C,O coordination mode occurs with a large distortion away from an ideal octahedral geometry at W, an effect driven by the acute bite angle of 60.9(1) ° of the chelating ligand.[20] This distortion also influences the geometry at the metallocarbene fragment. The W–C$^1$–O$^1$ and W–C$^1$–C$^2$ angles in **3a** are 115.4(2) and 130.0(3)°, close to the expected value for a sp$^2$-hybridised carbon center. Upon chelation to form **4a** these values become increasingly distorted away from an ideal geometry with the W–C$^1$–O$^1$ angle expanding to 141.3(2)° and W–C$^1$–C$^2$ angle contracting to 99.4(2)° (Figure 1b).

Complex **4a** reacts with $H_2$. Treatment of a benzene solution of **4a** with $H_2$ (1 atm.) at 100 °C for 2 h led to the corresponding F–T type product **5a** in >95 % NMR yield (Scheme 1). Attempts to crystallise this complex were unsuccessful, however compound **5a** was characterised by diagnostic resonances at $\delta = 4.38$ ppm and $\delta = 67.9$ ppm, in the $^1$H and $^{13}$C NMR spectra respectively, assigned to the new methylene group formed upon $H_2$ addition. Further analysis of the reaction mixtures revealed [W(CO)$_6$] and [W(CO)$_3$($\eta^6$-C$_6$D$_6$)] as side products of hydrogenation. An isotope labelling experiment in which **4a** was reacted with $D_2$ provided clear evidence for the formation of **5a**-$D_2$ with the methylene group resonating at $\delta = 4.38$ ppm in the $^2$H NMR spectrum. Hydrogenation of **3a** also directly leads to **5a**,[21] as does the reaction of **2**, $H_2$ and benzophenone at 100 °C.

The reaction scope was developed further (Figure 2). A series of C$_4$ homologation complexes (**3b–e**) were prepared from the reaction of **2** with CO,[18] 3-methylbenzaldehyde, 2-butanone, and 2,6-dimethylphenyl isocyanide. These reactions proceeded smoothly in all cases demonstrating that C$_3$→C$_4$ chain growth is possible with a range of electrophiles. Hydrogenation of **3b–e** led to **5b–e** in 60–95 % NMR yield. In the case of **3e**, the expected hydrogenation product can be observed spectroscopically but isomerizes to a more stable enamine tautomer under the reaction conditions. The reaction is not limited to C$_4$ homologation products, as direct hydrogenation of **2** was also possible leading to the formation of the C$_3$ analogue **5f**. Remarkably, **5b** could also be obtained in 50 % NMR yield from a direct reaction of [W(CO)$_6$], **1** and syngas (1:1 mixture of $H_2$/CO, 1 atm.) after 10 days at 100 °C. While the reaction is slow, this experiment shows that there is self-organisation in this system as F–T type products to be formed in a single step from simple starting materials.

Further experiments and calculations were undertaken to gain insight into the key hydrogenation step. The reaction of **3a** with $H_2$ (1 atm.) in benzene-$d_6$ at 100 °C was monitored as a function of time by in situ $^1$H NMR spectroscopy. Kinetic data show that hydrogenation of **3a** occurs as consecutive reactions with **4a** as intermediate (Supporting Information, Figure S6). Hydrogenation of **4a** was also monitored by $^1$H NMR spectroscopy. Kinetic data could be fitted to pseudo-1$^{st}$ order decay of [**4a**]. The rate constant for the $H_2$ reaction was found to be $k_{obs}(H_2) = 6.28\ (\pm 0.06) \times 10^{-4}$ s$^{-1}$ (Figure 3). Side-by-side kinetic runs with $H_2$ and $D_2$ gave a KIE of 1.02 (±0.01).

A series of plausible pathways for the hydrogenation reaction were calculated by DFT. The lowest energy path-

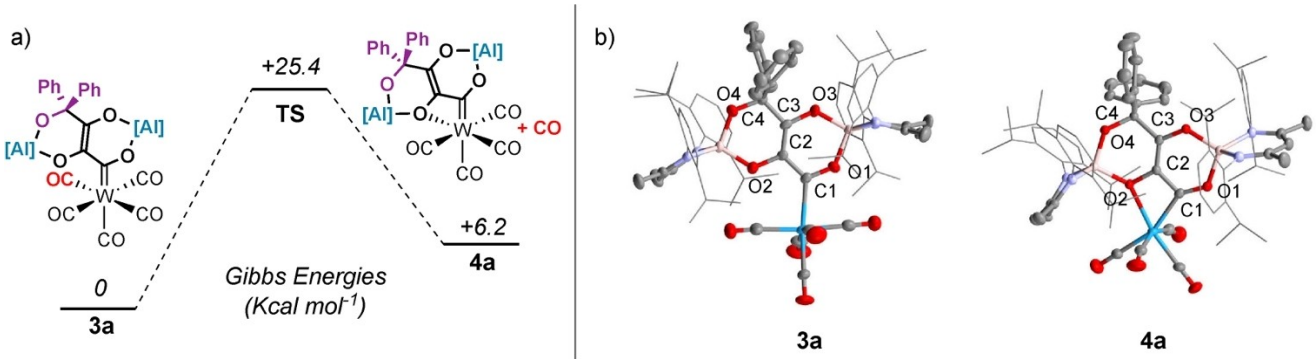


***Figure 1.*** a) DFT calculated mechanism for transformation of **3a** to **4a**. b) Solid-state structures of **3a** and **4a**.

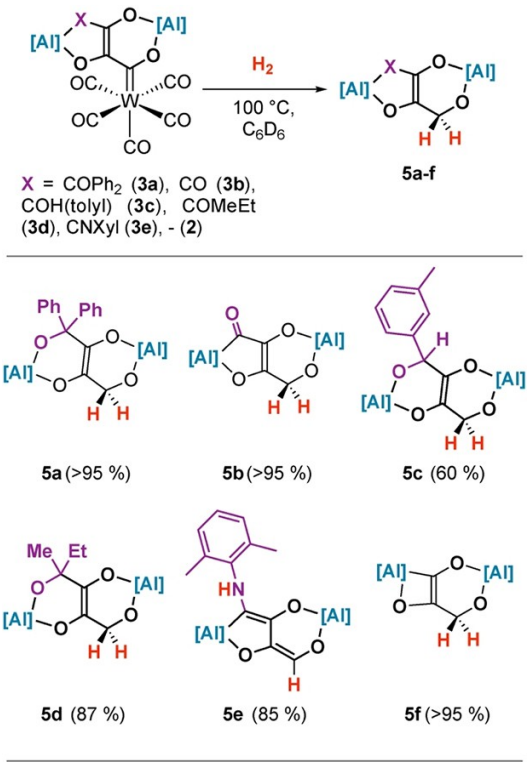


*Figure 2.* Scope of hydrogenation reaction. Yield determined by $^1$H NMR spectroscopy using 1,3,5-trimethoxybenzene as external standard.

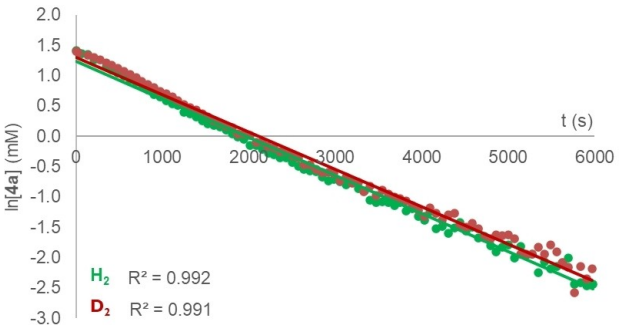


*Figure 3.* Ln[**4a**] versus time plot for reaction of **4a** with $H_2$ (green) and $D_2$ (red); $[\mathbf{4a}]_0 = 4.6$ mM.

way is depicted in Figure 4. The calculated mechanism is initiated by $\eta^2$-dihydrogen coordination to complex **4a** to give **Int-1**.[22–26] Formation of this intermediate occurs via an interchange mechanism ($\Delta G^{\ddagger}_{298K} = +21.7$ kcal mol$^{-1}$). Oxidative addition of $H_2$ to the W centre from **Int-1** gives the dihydride intermediate **Int-2** via a low energy barrier transition state **TS-2** followed by a barrierless migration of one of the hydrides to the carbon atom of the metallocarbene to give **Int-3**. There is precedent for this type of 1,2-migration involving hydride and metallocarbene ligands.[27–29] Prior calculations are consistent with a low energy process.[30–32] **Int-3** is stabilised by an agostic interaction of the newly formed C–H bond to W.[33] After two consecutive rotations steps via **TS-4** and **TS-5**, **Int-3** leads to **Int-5** which is stabilised by coordination of an oxygen atom of the carbon chain. **Int-5** dissociates a CO ligand through **TS-6** to give **Int-6. Int-6** then rotates again through **Int-7** to **Int-8** which is preorganised for reductive elimination via **TS-9** to afford the thermodynamically stabilised **Int-9**, a precursor of the final products.[34] The barrier for the

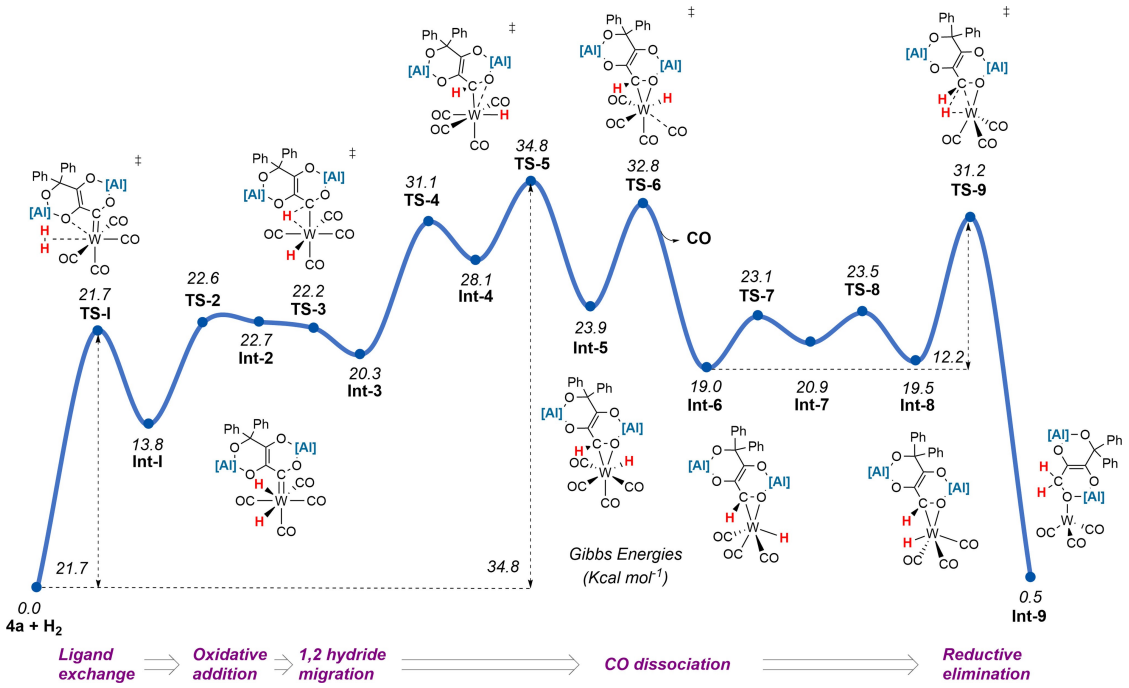


*Figure 4.* DFT-calculated mechanism for hydrogenation of **4a**.

reductive elimination step is low ($\Delta G^{\ddagger}_{298K} = +11.7$ kcal mol$^{-1}$).

Overall, this calculated mechanism proceeds via a series of established fundamental steps of organometallic compounds namely: i) ligand substitution, ii) oxidative addition, iii) migratory insertion, and iv) reductive elimination. The Gibbs activation energy corresponds to an energy span from **4a** to **TS-5** ($\Delta G^{\ddagger}_{298K} = +34.8$ kcal mol$^{-1}$).[35] The rate-limiting sequence involves coordination of $H_2$, oxidative addition of $H_2$, hydride migration from W to C and CO dissociation. The predicted pathway is consistent across a series of DFT functionals.

Consideration of the calculated reaction mechanism suggests that the assignment of a KIE in this system is complex. Although the experimentally determined KIE of 1.02 ($\pm$0.01) could be interpreted as a simple step not involving hydrogen atoms, based on the calculations it more likely arises from the combination of individual KIEs (or EIEs) from a series of steps. While oxidative addition of $H_2$ to W is expected to show a normal primary KIE, $H_2$ binding often occurs with an inverse IE.[36] Similarly, based on the stretching vibrational modes, hydride migration from W to C might be expected to occur with an inverse KIE.[37]

In summary, we report the formation of F–T type products from the combination of $H_2$, CO, organic electrophiles, and a main group reductant. The reaction scope allows the generation of both $C_3$ and $C_4$ chains with complete selectively. The hydrogenation step is mediated by the transition metal which likely plays a key role through activation of $H_2$ at a site adjacent to a metallocarbene ligand. These findings greatly expand the scope and understanding of reactivity for homogeneous systems reported that combine $H_2$ and CO to make hydrogenated carbon chains.

Crystal data is available through the CCDC.[38] Primary data (.mnova, .txt and .xyz) are available from Imperial's Research Data Repository and available through the following link: 10.14469/hpc/10042.

## Author Contributions

M.B. and R.Y.K. carried out the experimental work. M.B. carried out the calculations. A.J.P.W. and R.Y.K. performed the crystallography. R.Y.K. designed the initial experiments and M.B. advanced the ideas. M.B. and M.R.C. wrote the manuscript with feedback from all authors. All authors have given approval to the final version of the manuscript.

## Acknowledgements

We thank Imperial College London for the award of a President's Scholarship (R.Y.K.). We also thank the EPSRC for project funding (EP/S036628/1).

## Conflict of Interest

The authors declare no conflict of interest.

## Data Availability Statement

The data that support the findings of this study are openly available in Imperial's Research Data Repository at 10.14469/hpc/10042, reference number 10042.

**Keywords:** CO · Fischer–Tropsch · Homologation · Metallocarbenes · Reaction Mechanisms

[1] H. Schulz, *Appl. Catal. A* **1999**, *186*, 3–12.
[2] A. De Klerk, *Kirk-Othmer Encyclopedia of Chemical Technology, Fischer–Tropsch Process 1*, Wiley, Hoboken, **2013**; pp. 1–36.
[3] R. B. Anderson, R. A. Friedel, H. H. . Storch, *J. Chem. Phys.* **1951**, *19*, 313–319.
[4] N. M. West, A. J. M. Miller, J. A. Labinger, J. E. Bercaw, *Coord. Chem. Rev.* **2011**, *255*, 881–898.
[5] R. Y. Kong, M. R. Crimmin, *Dalton Trans.* **2020**, *49*, 16587–16597.
[6] B. D. Dombek, *Adv. Catal.* **1983**, *32*, 325–416.
[7] J. A. . Labinger, *J. Organomet. Chem.* **2017**, *847*, 4–12.
[8] P. M. . Maitlis, *J. Organomet. Chem.* **2004**, *689*, 4366–4374.
[9] Z. Qi, L. Chen, S. Zhang, J. Su, G. A. Somorjai, *Top. Catal.* **2020**, *63*, 628–634.
[10] G. C. Demitras, E. L. Muetterties, *J. Am. Chem. Soc.* **1977**, *99*, 2796–2797.
[11] M. Yalpani, R. Köster, *J. Organomet. Chem.* **1992**, *434*, 133–141.
[12] H. Braunschweig, T. Dellermann, R. D. Dewhurst, W. C. Ewing, K. Hammond, J. O. C. Jimenez-Halla, T. Kramer, I. Krummenacher, J. Mies, A. K. Phukan, A. Vargas, *Nat. Chem.* **2013**, *5*, 1025–1028.
[13] B. Wang, G. Luo, M. Nishiura, Y. Luo, Z. Hou, *J. Am. Chem. Soc.* **2017**, *139*, 16967–16973.
[14] J. D. Protasiewicz, S. J. Lippard, *J. Am. Chem. Soc.* **1991**, *113*, 6564–6570.
[15] D. L. M. Suess, J. C. Peters, *J. Am. Chem. Soc.* **2013**, *135*, 12580–12583.
[16] S. Hu, T. Shima, Z. Hou, *J. Am. Chem. Soc.* **2020**, *142*, 19889–19894.
[17] M. Xu, Z. W. Qu, S. Grimme, D. W. Stephan, *J. Am. Chem. Soc.* **2021**, *143*, 634–638.
[18] R. Y. Kong, M. R. Crimmin, *J. Am. Chem. Soc.* **2018**, *140*, 13614–13617.
[19] R. Y. Kong, M. Batuecas, M. R. Crimmin, *Chem. Sci.* **2021**, *12*, 14845–14854.
[20] I. J. Hart, J. C. Jeffery, R. M. Lowry, F. G. A. Stone, *Angew. Chem. Int. Ed. Engl.* **1988**, *27*, 1703–1705; *Angew. Chem.* **1988**, *100*, 1769–1775.
[21] To check if insertion could occur also into hydrogenated products, reaction of **3a** with benzophenone was tested and no reactivity was observed, suggesting that the reaction follows the sequence insertion–hydrogenation.
[22] Although different geometries for **Int-1** can be proposed, rotational barriers for $H_2$ ligand have been calculated to be low in energy for this molecule ($\Delta G^{\circ}_{298K} = +3.2$–$6.8$ kcal mol$^{-1}$ and $\Delta G^{\ddagger}_{298K} = +0.7$–$4.5$ kcal mol$^{-1}$) and are in agreement with previous results for related molecules (see Supporting Information).
[23] P. J. Hay, *J. Am. Chem. Soc.* **1987**, *109*, 705–710.
[24] P. J. Hay, *Chem. Phys. Lett.* **1984**, *103*, 466–469.
[25] J. Eckert, J. H. Kubas Hall, P. J. Hay, C. M. Boyle, *J. Am. Chem. Soc.* **1990**, *112*, 2324–2332.
[26] T. A. Albright, *Acc. Chem. Res.* **1982**, *15*, 149–155.

[27] V. A. Osborn, C. A. Parker, M. J. Winter, *J. Chem. Soc. Chem. Commun.* **1986**, 1185–1186.
[28] C. P. Casey, S. M. Neumann, *J. Am. Chem. Soc.* **1977**, *99*, 1651–1652.
[29] J. C. Green, M. L. H. Green, C. P. A. Morley, *Organometallics* **1985**, *4*, 1302–1305.
[30] E. A. Carter, W. A. Goddard III, *J. Am. Chem. Soc.* **1987**, *109*, 579–580.
[31] T. Ziegler, L. Versluis, V. Tschinke, *J. Am. Chem. Soc.* **1986**, *108*, 612–617.
[32] E. A. Carter, W. A. Goddard, *Organometallics* **1988**, *7*, 675–686.
[33] Alternative mechanisms in which **Int-1** undergoes CO dissociation to give a pentacoordinated dihydrogen intermediate or in which CO dissociation and H migration occur simultaneously from **Int-2** have been discarded due to their high transition state energy: **TS-2a**, $\Delta G^{+}_{298K} = +42.3\ kcal\,mol^{-1}$; **TS-3b**, $\Delta G^{+}_{298K} = +44.0\ kcal\,mol^{-1}$ (see Supporting Information).
[34] An alternative plausible mechanism from **Int-5** in which CO dissociation does not take place was calculated to present a similar energy ($\Delta G^{+}_{298K} = +35.9\ kcal\,mol^{-1}$) (see Supporting Information).
[35] The energy span from **4a** to **TS-6** ($\Delta G^{+}_{298K} = +32.8\ kcal\,mol^{-1}$) is similar. These two steps are close in energy and either could be rate-limiting.
[36] K. E. Janak, G. Parkin, *Organometallics* **2003**, *22*, 4378–4380.
[37] R M. Bullock, B. R. Bender, *Encyclopedia of Catalysis, Isotope Methods—Homogeneous* (Ed.: I. Horváth), Wiley, Hoboken, **2000**, pp. 1–62.
[38] Deposition numbers 2130349, 2130350, 2130351, 2129490, 2129491, 2129492 contain the supplementary crystallographic data for this paper. These data are provided free of charge by the joint Cambridge Crystallographic Data Centre and Fachinformationszentrum Karlsruhe Access Structures service.

Manuscript received: February 10, 2022
Accepted manuscript online: February 28, 2022
Version of record online: March 16, 2022